

# UCLA

## UCLA Previously Published Works

### Title

Control of residual aluminum from conventional treatment to improve reverse osmosis performance

### Permalink

<https://escholarship.org/uc/item/7q66f96m>

### Journal

Desalination, 190(1-3)

### ISSN

0011-9164

### Authors

Gabelich, C J  
Ishida, K P  
Gerringer, F W  
[et al.](#)

### Publication Date

2006-04-01

Peer reviewed

## Control of Residual Aluminum from Conventional Treatment To Improve Reverse Osmosis Performance

Christopher J. Gabelich<sup>a\*</sup>, Kenneth P. Ishida<sup>b</sup>, Fredrick W. Gerringer<sup>a</sup>,  
Ray Evangelista<sup>c</sup>, Minhaal Kalyan<sup>c</sup>, I.H. “Mel” Suffet<sup>d</sup>

<sup>a</sup>Metropolitan Water District of Southern California, La Verne, California  
Tel. +1(909)392-5113; Fax +1(909)392-5166; email: cgabelich@mwdh2o.com

<sup>b</sup>Orange County Water District, Fountain Valley, California

<sup>c</sup>California State Polytechnic University, Pomona, California

<sup>d</sup>University of California at Los Angeles, Los Angeles, California

### ABSTRACT

Soluble aluminum ( $Al^{3+}$ ) may react with both ambient silica and antiscalant components to form colloidal foulants during reverse osmosis (RO) treatment. Whereas conventional treatment (coagulation/filtration/sedimentation/dual-media filtration) was being used prior to RO, aluminum sulfate (alum) and polyaluminum chloride (PACl) coagulants were evaluated at ambient pH (pH 7.8 to 7.9) and suppressed pH (pH 6.7) in an effort to lower the total aluminum to below 50  $\mu\text{g/L}$ —a level previously observed to prevent RO membrane fouling. Additional tests were conducted with 5 mg/L citric acid added to the RO influent to chelate the soluble aluminum fraction. All tests were conducted with 1.5 to 2.5 mg/L chloramines present. Testing of a RO process fed with optimized alum- or PACl-coagulated water showed that PACl outperformed alum regardless of pH. Alum coagulation at ambient pH resulted in 184 to 273  $\mu\text{g/L}$  total aluminum passing through the filtration process. Only by lowering the mean influent water pH to 6.7 was the mean soluble aluminum residual (45  $\mu\text{g/L}$ ) for alum coagulation reduced to below the 50  $\mu\text{g/L}$  aluminum goal. Regardless of pH, for alum-coagulated waters, the higher aluminum carryover resulted in severe RO membrane fouling within 500 hours of operation. Only when a chelating agent (citric acid) was added to the RO feed was the loss in productivity and selectivity arrested. However, PACl consistently met the 50- $\mu\text{g/L}$  goal for both total and soluble aluminum for all pH levels tested, which resulted in more stable membrane performance over time. Further research on the compatibility of PACl and polyamide membranes in the presence of chloramines is needed as data from this project suggest PACl coagulation may facilitate membrane oxidation.

*Keywords:* Reverse osmosis, alum, polyaluminum chloride, aluminum, fouling

---

\* Corresponding author.

## INTRODUCTION

Previous research conducted by the Metropolitan Water District of Southern California (MWDSC) identified aluminum silicate-based, aluminum hydroxide-based, and aluminum phosphate-based fouling during reverse osmosis (RO) treatment [1]. Each of these foulants presumably resulted from excessive aluminum introduced into the RO feed water by the use of aluminum sulfate (alum) during the upstream coagulation process. Based on typical alum dosages at MWDSC treatment plants and aluminum's inherent solubility, up to 200 µg/L of total aluminum has been measured at the filter effluent. Despite these limitations, pretreatment using conventional treatment (i.e., coagulation, flocculation, sedimentation, multi-media filtration) is desirable to reduce the costs of potentially implementing RO technology at one or more of MWDSC's treatment plants.

This paper presents pilot-scale results evaluating two aluminum-based coagulants (alum and polyaluminum chloride [PACl]) in an attempt to reduce the total aluminum residual from the filter effluent to less than 50 µg/L while still maintaining a low-turbidity effluent (less than 0.3 NTU for 95th percentile data) [2]. By reducing the aluminum content of the RO feed water to less than 50 µg/L, fouling problems associated with conventional pretreatment may be alleviated. This work may also help utilities comply with the draft public health goal for aluminum in California (60 µg/L) [3] without resorting to more corrosive coagulants such as ferric chloride or ferric sulfate.

## BACKGROUND

The accumulation of particles (e.g., fine clays, silts, and inorganic hydroxides) on a RO membrane increases the resistance across the membrane over time, resulting in a reduction of permeate flux, or water production [4]. Thus, maintaining high flux rates in downstream membrane processes requires effective pre-treatment for particle removal. Coagulation processes, though efficient in achieving turbidity removal, are known to have coagulant "carryover" or residuals [5]. Potential methods to minimize coagulant residuals include coagulant dose optimization, pH control, alternative coagulant selection, or additional chemical additives.

## Previous Research

Previous research conducted at MWDSC using Colorado River water has identified aluminum hydroxide, aluminum silicate, and aluminum phosphate-based fouling during reverse osmosis (RO) treatment (Figure 1) [1,6]. Each of these foulants was presumably caused by excessive aluminum introduced into the RO feed water by the use of aluminum sulfate (alum) coagulation upstream, which imparts up to 200 µg/L of total aluminum at the filter effluent.

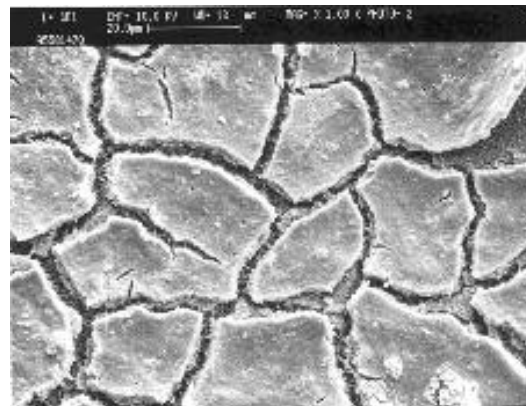
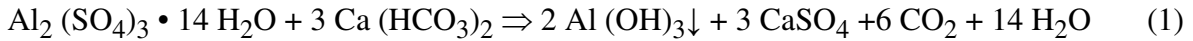


Figure 1. Scanning electron micrograph of aluminum silicates on polyamide membrane surface. 5000x magnification [6].

Aluminum hydroxides are formed when alum ( $\text{Al}_2(\text{SO}_4)_3 \cdot 14 \text{H}_2\text{O}$ ) is added to water containing natural alkalinity via the following general reaction [7]:



The main coagulation mechanism for alum is the dissociation of positively charged aluminum ions. Based on solution pH, however, various aluminum polymers and monomers are possible (Figure 2). At the pH ranges observed at MWDSC's treatment plants (pH 7.5–8.5), aluminum is primarily found in the form  $\text{Al}(\text{OH})_4^-$ . Other forms of hydrated aluminum, however, include  $\text{AlOH}^{2+}$ ,  $\text{Al}(\text{OH})_2^+$ ,  $\text{Al}_3(\text{OH})_4^{5+}$ , and  $\text{Al}_{13}\text{O}_4(\text{OH})_{24}^{7+}$  [8]. Although experimental evidence confirms the existence of polynuclear  $\text{Al}_{13}$ , there is doubt that “giant” cations such as  $\text{Al}_{13}\text{O}_4(\text{OH})_{24}^{7+}$  are present in alum-coagulated waters [9]. Aluminum present during alum coagulation is least soluble from pH 5.7 to 6.2 [9].

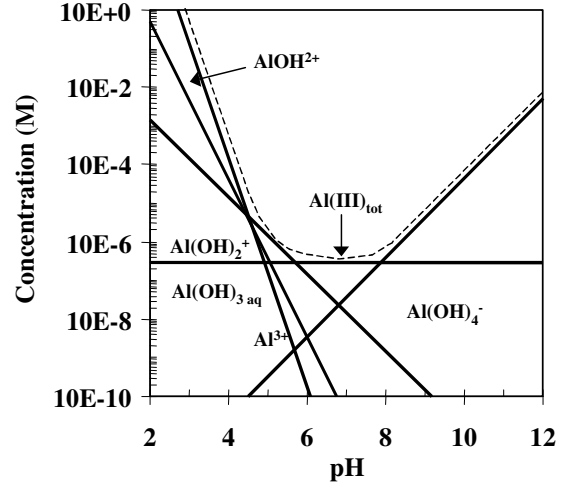
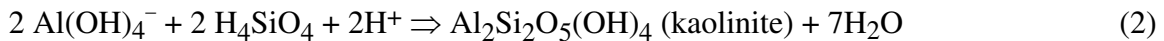


Figure 2. Solubility of monomeric aluminum [8].

Whereas colloidal aluminum silicates such as kaolinite are readily removed during the conventional treatment process, they can reform within the RO system via the following reaction [1]:



Many antiscalants designed to control for silica scaling are ineffective against aluminum silicates [10,11]. In addition, phosphorous (a key inorganic component in many antiscalant formulations) can react with excess aluminum [12]. The basic reaction involved in the precipitation of phosphorus and aluminum follows:



The solubility of  $\text{AlPO}_4$  is a direct function of pH, with  $\text{AlPO}_4$  being less soluble at pH 6.5 than pH 8.5 [12].

An alternative aluminum-based polymer is “polyaluminum chloride,” a term that refers to a class of compounds with the general formula  $\text{Al}_2(\text{OH})_x\text{Cl}_y$ , with  $x$  and  $y$  dependent on Al:Cl molar ratio. As the chlorine content decreases, the degree of neutralization ( $r$ ), or basicity, increases. Basicity can be characterized by the following formulas [13, 14]:

$$r = \text{OH}/\text{Al} \quad (4)$$

where:  $\text{basicity} = (r/3) \times 100 \quad (5)$

PACl consists of preformed polymers of varying lengths, distinct from alum that mainly consists of monomers [15]. The dominant polymer in high-basicity PACl is  $\text{Al}_{13}\text{O}_4(\text{OH})_{24}^{7+}$  [16,17]. As the degree of basicity increases, so too does the proportion of  $\text{Al}_{13}^{+}$  polymers. Aluminum chlorohydrate (ACH) is a specific type of PACl with an Al:Cl ratio of 2:1 and a basicity of 83 percent. The common chemical formula for ACH is  $\text{Al}_2(\text{OH})_5\text{Cl}$  [13]. For ACH, aluminum solubility between pH 7.0 and pH 10 is fairly constant. Below pH 7.0, however, aluminum solubility increases sharply (Figure 3) [16]. In general, ACH

### Mitigation Strategies

Strategies for avoiding precipitative scaling often include reducing the concentration of either the anion or the cation portion of the salt of concern [18,19]. Although phosphate solubility is pH-sensitive, silica solubility is fairly insensitive at the pH ranges observed during conventional water treatment (i.e., pH 6.5–8.5) [20]. Therefore, to prevent both aluminum silicate and aluminum phosphate fouling/scaling, control of the residual aluminum concentration is beneficial. Monomeric aluminum solubility (i.e., during alum coagulation) is fairly sensitive to pH adjustment (Figure 2), though the speciation changes from  $\text{Al}(\text{OH})_4^-$  (pH 8.5) to  $\text{Al}^{3+}$  (pH 6.0). In contrast, aluminum solubility for polymerized aluminum (i.e., during PACl coagulation) is fairly stable above pH 7.0, though published data indicated that aluminum solubility increased dramatically below pH 7.0 (Figure 3) [16]. Therefore, pH control may have a differing effect on aluminum concentration depending on coagulant type. Results from MWDSC demonstrated that PACl consistently met the 50  $\mu\text{g}/\text{L}$  aluminum goal regardless of pH (pH 6.0–8.3), whereas alum could only meet the goal for soluble aluminum below pH 6.5 [21]. For total aluminum, alum coagulation between pH 6.0–8.3 failed to meet the 50  $\mu\text{g}/\text{L}$  goal, which may result in colloidal fouling of any downstream membrane.

Chelating agents such ethylenediaminetetraacetic acid (EDTA), citric acid, and acetic acid have been suggested to inhibit aluminum silicate scale formation [22,23,24]. Research at MWDSC demonstrated that EDTA and citric acid effectively chelated residual aluminum during alum coagulation [1]. Whereas dispersant agents containing phosphonic acid and/or phosphonate functional groups may inhibit pure amorphous silica, they can potentially precipitate as aluminum phosphates or phosphonates; thus, they may act as foulants themselves.

should result in a lower aluminum residual than alum.

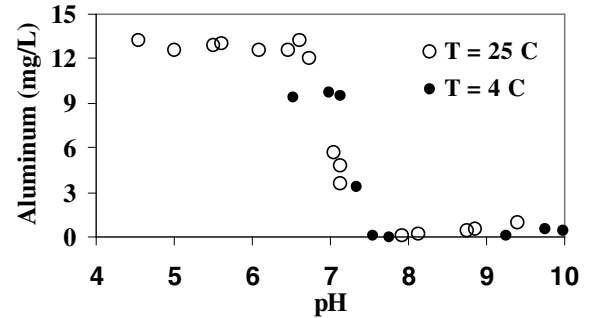


Figure 3. Aluminum solubility using PACl ( $5.04 \times 10^{-4}$  M  $\text{Al}^{3+}$ , 83% basicity) in deionized water at two temperatures. Adapted from [16].

## EXPERIMENTAL METHODS

Seven tests were conducted for this study. Table 1 lists the experimental conditions for each test. The pretreatment/RO process consisted of two trains (Trains A and B), which were operated in parallel for the first three runs (Tests #1 through #6) and with only Train A for the fourth run (Test #7). A summary of influent water quality data for all tests is presented in Table 2. For the duration of pilot-scale testing, the source water was a blend of Colorado River water and California State Water Project water—an operational constraint at MWDSC’s research facility in La Verne, California. Although the salinity of the source water was lower than that of Colorado River water, the treatability in terms of chlorine demand and coagulation chemistry should be comparable.

Table 1. Experimental Matrix

Test #	Description	Train
1	10 mg/L Alum & 2 mg/L polyDADMAC at pH 7.9	A
2	2 mg/L PACl & 2 mg/L polyDADMAC at pH 7.9	B
3	10 mg/L Alum & 2 mg/L polyDADMAC at pH 6.7	A
4	2 mg/L PACl & 2 mg/L polyDADMAC at pH 6.7	B
5	10 mg/L Alum & 2 mg/L polyDADMAC at pH 7.8 with 5 mg/L citric acid	A
6	10 mg/L Alum & 2 mg/L polyDADMAC at pH 7.8 with 5 mg/L citric acid and 3 mg/L antiscalant	B
7	2 mg/L PACl & 2 mg/L polyDADMAC at pH 7.8 with 5 mg/L citric acid	A

### Pilot-Scale Treatment Plant

A dual-train conventional filtration (rapid mix/flocculation/sedimentation/filtration) treatment plant with a combined flow rate of 9 gpm [34 L/min] was used for this study. Coagulant addition ranged from 7.5 to 10 mg/L alum ( $\text{Al}_2(\text{SO}_4)_3 \cdot 14 \text{H}_2\text{O}$ , Rhodia Inc., Cranbury, New Jersey) or 2.0 mg/L PACl or ACH (Sumalchlor 50, Summit Research Labs, Flemington, N.J.) and 2.0 mg/L cationic polymer (polydimethyldiallyl ammonium chloride [polyDADMAC], NS 3150, Neo Solutions, Inc., Beaver, Pa.). A 1.5–2.5 mg/L free chlorine residual was maintained at the filter influent and converted to chloramines through ammonium sulfate addition (3:1 chlorine to ammonia w/w ratio). Influent water was pH adjusted with sulfuric acid (66° Bé, Spectrum Quality Products, Inc., Gardena, Calif.).

Table 2. Mean influent water quality data for pilot-scale testing

Parameter (mg/L)	Value
Total dissolved solids	391 (28)
Total hardness as $\text{CaCO}_3$	176 (11)
Total alkalinity as $\text{CaCO}_3$	93 (11)
Total organic carbon	2.6 (0.4)
Calcium	40 (3.2)
Magnesium	17 (2.9)
Sulfate	122 (17)
Fluoride	0.2 (0.0)
Silica	12 (0.6)
Aluminum ( $\mu\text{g/L}$ ) [Total]	48 (26)
Aluminum ( $\mu\text{g/L}$ ) [Soluble]	27 (23)

Data in parentheses indicate standard deviation.

Filter media was 18-in. anthracite coal over 8-in. sand. The dual-media filters were backwashed based on the following criteria: (1) effluent turbidity (Hach 2100N Turbidimeter, Hach Company, Loveland, Colo.) levels exceed 0.3 NTU; (2) terminal headloss accumulation (6 ft [1.8 m]), or (3) 12-h filter run time. The filtration rate was less than 6.0 gpm/ft<sup>2</sup> [0.2 m/min].

### **Pilot-Scale Reverse Osmosis Units**

Identical two-element membrane-test units (Nimbus 2500, Nimbus Water Systems, San Marcos Calif.) were pilot tested during this project. Each unit had two 2 1/2-in. × 40-in. membrane elements (2540 TFC-ULP<sup>®</sup>, Koch Membrane Systems, San Diego, Calif.) in series. Throughout the experiments, the operating flux ( $5.7 \times 10^{-6}$  m/s) and water recovery (15 percent) were kept constant by adjusting the feed pressure (550 to 830 kPa). Silt density index (SDI) was measured using the method described by the American Society for Testing and Materials (ASTM) method D 4189–82 [25]. Membrane flux and salt rejection were normalized to 25°C per ASTM method D 4516–85 [26]. Citric acid (technical grade, Spectrum Chemicals, Gardena, Calif.) and an antiscalant (Flocon 100, GE Osmotics, Minnetonka, Minn.) were dosed at 5.0 mg/L and 3.0 mg/L, respectively.

### **Analytical Methods**

Alkalinity, hardness, major cations and anions, total dissolved solids (TDS), trace metals, turbidity, temperature, and pH were measured per *Standard Methods for the Examination of Water and Wastewater* [27]. The aluminum content from the raw and filtered water was subdivided into total and soluble fractions [5]. The soluble fraction was defined as that material not retained by a 0.45 µm filter (ZapCap CR 0.45 micron nylon, VWR Scientific Products, San Diego, Calif.). All aluminum samples were analyzed in accordance with EPA Method 200.8 using a Perkin-Elmer Elan 6000 ICP-MS (method reporting limit [MRL], 5 µg/L).

Scanning electron microscopy (SEM) was conducted using a Phillips XL30-FEG (Phillips, Natick, Mass.) with energy-dispersive spectroscopy (EDS) (EDAX, Mahwah, New Jersey) capabilities per Goldstein et al. [28]. The EDS were conducted on 20 × 20 µm samples at 15 kV accelerating voltage and all data are given in percent weights of detected elements greater than 16 atomic mass units. Membrane fouling was also detected through attenuated total reflectance Fourier-transform infrared (ATR/FT-IR) spectroscopy using a Magna 550 spectrometer (Thermo Nicolet, Madison, Wisc.) utilizing GRAMS/AI software (Version 7.00, Thermo Galactic, Salem, N.H.) [29].

## **RESULTS AND DISCUSSION**

Figure 4 shows pretreatment effluent water quality data for turbidity (NTU), SDI, and residual aluminum (µg/L) at pHs 7.9, 7.8, and 6.7. Whereas, for all intents and purposes, pH 7.9 and 7.8 are statistically identical, these tests were run at different times and included different chemical additives (e.g., citric acid and antiscalant) prior to RO treatment; hence these data are presented separately. In terms of turbidity, PACl showed lower filter effluent median turbidity and generally tight data ranges (minimum to maximum) than alum-treated waters regardless of solution pH. Silt density indices were comparable for the two coagulant-treated waters throughout testing. However, SDI data for both alum and PACl were statistically higher at pH

6.7 than for pH 7.9. Figure 4 also shows alum coagulation at pH 7.9 resulted in 184 to 273  $\mu\text{g/L}$  total aluminum to pass through the filtration process—more than 3 times the target goal of 50  $\mu\text{g/L}$ . Lowering the mean influent water pH to 6.7 reduced the mean soluble aluminum residual (45  $\mu\text{g/L}$ ) for alum to below the 50- $\mu\text{g/L}$  aluminum goal (Figure 4). However, PACl consistently met the 50  $\mu\text{g/L}$  goal for both total and soluble aluminum for all pH levels tested, although data from pH 6.7 was significantly higher than at pH 7.9. Coagulant doses for alum (10 mg/L) and PACl (2.0 mg/L) remained constant regardless of solution pH. All tests included 2.0 mg/L polyDADMAC co-polymer.

Of the four variables studied (filter effluent turbidity, SDI, and total and soluble aluminum), coagulant selection and solution pH had the greatest affect on the residual aluminum (both total and soluble). Figure 5 shows the effect of residual aluminum on specific flux (m/s/kPa), salt rejection (percent), and differential pressure (kPa) of polyamide membranes operated at pH 7.9, 7.8, and 6.7 using alum and PACl coagulation. All RO data was normalized to 25°C.

After less than 450 hrs of run time, the specific flux data for alum pretreated membranes at pH 7.9 and 6.7 showed marked decreases in specific flux (50 and 40 percent, respectively) and decreases in salt rejection (2 percent for both data sets) (Figure 5). These data suggest severe colloidal aluminum fouling of the membrane surfaces (see following discussion on EDS data from more details). The decline for alum at pH 6.7 was significantly less than that at pH 7.9. The addition of citric acid to the alum feed (pH 7.8) lessened the degree of specific flux loss and halted the increase in salt passage, whether or not an antiscalant was also added. In-house data using alum coagulation without citric acid showed enhanced colloidal fouling when using polycarboxylic acid-based antiscalants [30]. These data refute previous bench-scale data, which showed that, although chelating agents (e.g., citric acid) may be effective in halting aluminum silicate formation, the beneficial effect was lost upon the addition of a phosphonate-based antiscalant [1].

The PACl-pretreated membranes at pH 7.9 and 6.7 exhibited no losses in specific flux and only slight declines (0.5 percent) in salt rejection over time (Figure 5). Relative values for differential pressure—a measure of hydraulic resistance tangentially across the RO elements—between alum and PACl were consistent over time, indicating minimal feed spacer blinding caused by colloidal particle deposition. Numerical differences in differential pressures between coagulants were a function of the treatment train (i.e., either Train A or B) from which the data were collected, rather than the coagulant itself. Previous research has shown a decrease in salt rejection accompanied by a loss in membrane productivity (i.e., flux) without increasing the differential pressure is attributed to cake-enhanced osmotic pressure [31, 32]. In contrast, increases in membrane productivity with a concomitant decrease in salt rejection are the hallmarks of membrane oxidation [6, 33]. The high basicity of the PACl used during this study may have facilitated the decomposition of  $\text{NH}_2\text{Cl}$ , which resulted in enhanced membrane oxidation through the formation of an amidogen radical [33]. The addition of 5-mg/L citric acid did stabilize both specific flux and salt rejection for the PACl/polyDADMAC exposed membrane, suggesting that the sequestration of the aluminum may halt any potential membrane oxidation. This potential phenomenon was not formally addressed during this study and warrants further investigation.



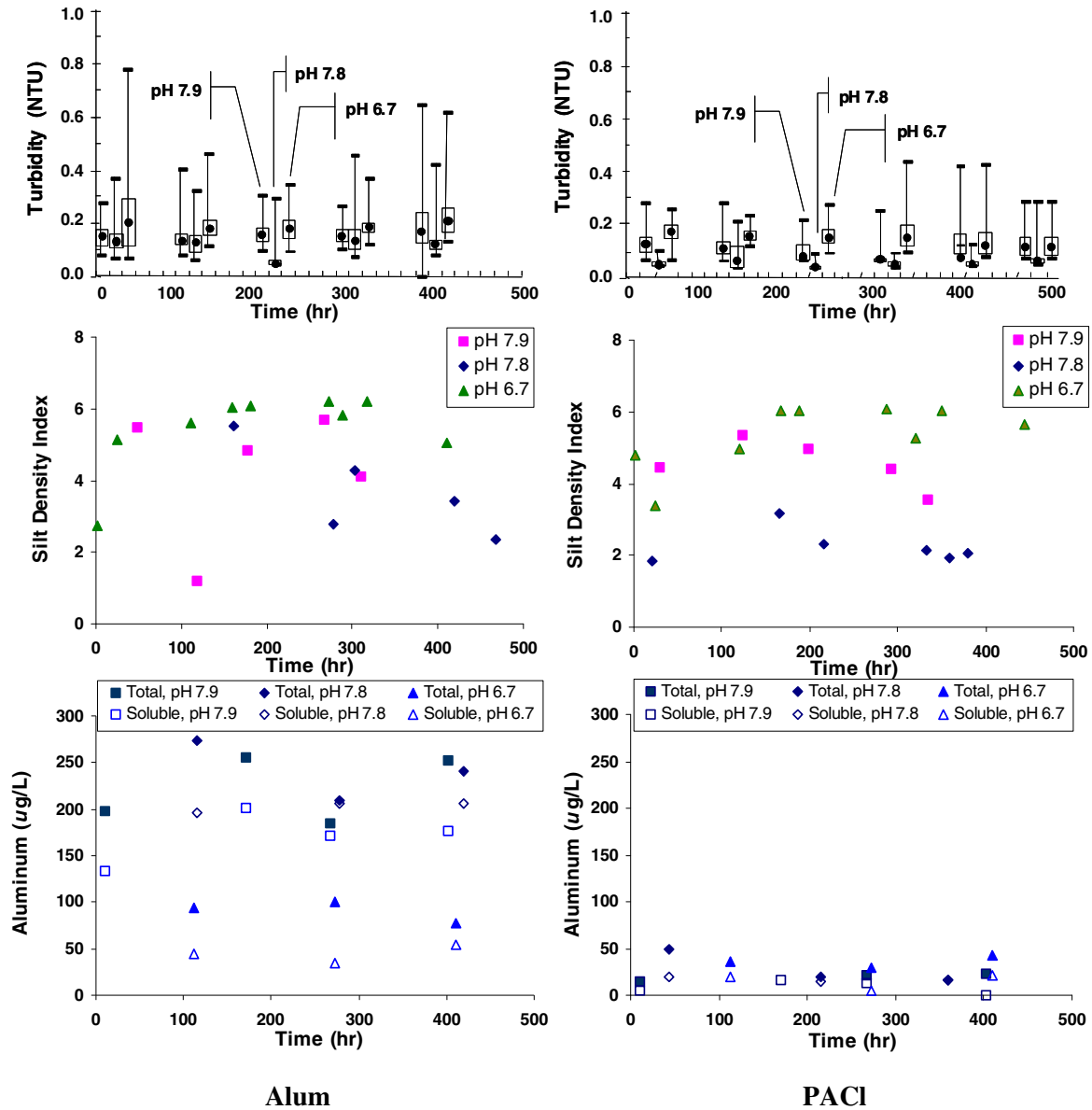


Figure 4. Pretreatment effluent water quality after alum/polyDADMAC (left column) and PACl/polyDADMAC (right column) coagulation: turbidity (top row), silt density index (middle row), and residual aluminum (bottom row). Box-and-whisker plots show maximum, 75th percentile, median, 25th percentile, and minimum data.

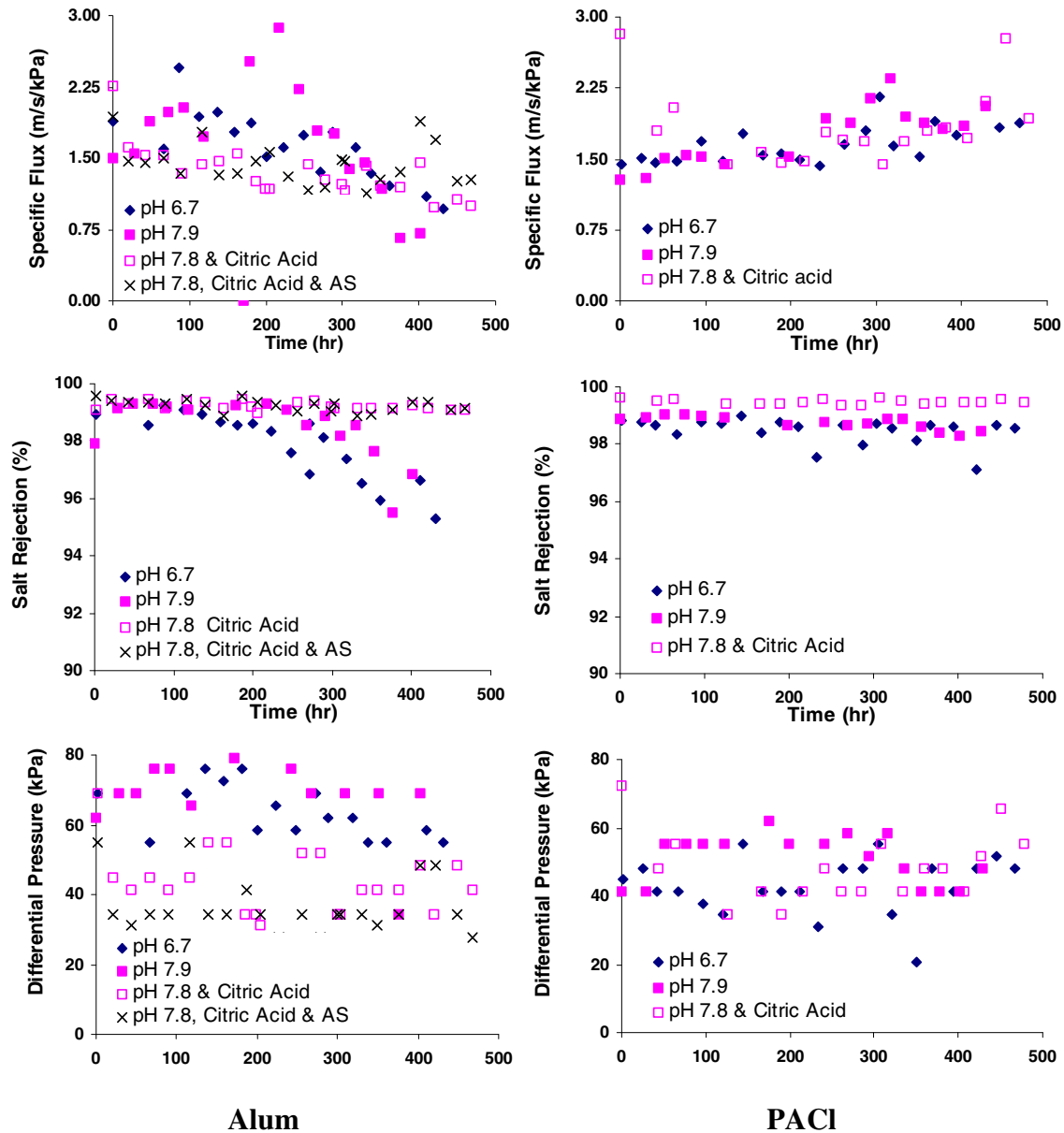


Figure 5. Specific flux (m/s/kPa), salt rejection (percent), and differential pressure (kPa) of polyamide membranes operated using alum/polyDADMAC (left column) and PACI/polyDADMAC (right column) coagulation. All data normalized to 25°C.

After each run, all RO elements were removed and the lead elements were autopsied. Visually, alum-treated membranes had a slippery, gelatinous red-brown fouling layer deposited on the surface. All PACI-treated membranes (pH 7.9, 7.8, and 6.7) had only minimal amounts of foulants deposited on the surface. Figure 6 and Table 3 show the ATR/FT-IR and EDS data from the polyamide membrane surfaces, respectively. Figure 7 shows the scanning electron micrographs of the membranes operated under the various experimental conditions.

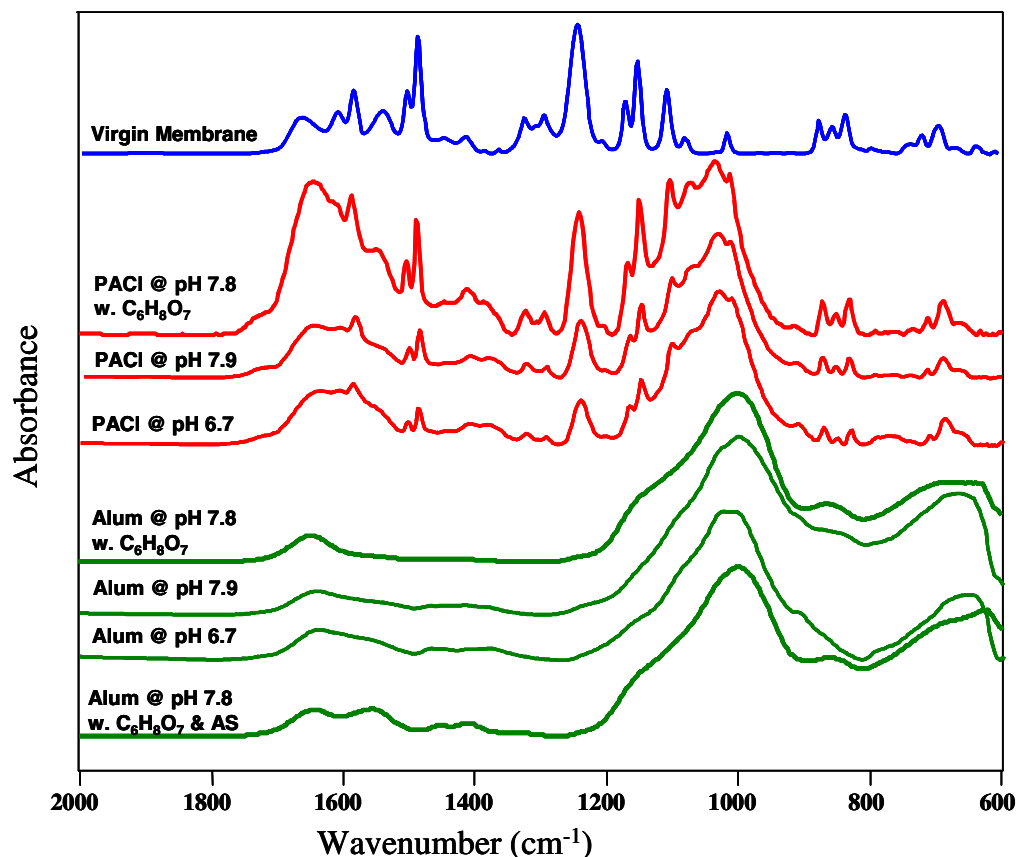


Figure 6. ATR/FT-IR spectra of polyamide membranes exposed to alum/polyDADMAC and PACI/polyDADMAC. AS = Flocon 100 antiscalant.

The ATR/FT-IR spectrum of the polyamide membrane is dominated by vibrational bands of the polysulfone support membrane with major bands at 1586, 1503, 1488 and 1242  $\text{cm}^{-1}$  (Figure 6). The major vibrational bands associated with the thin polyamide layer are the amide I (C=O) near 1660  $\text{cm}^{-1}$  and the amide II (N-H) near 1540  $\text{cm}^{-1}$ . Other bands at 1607, 1488, and 1448  $\text{cm}^{-1}$  are associated with the C=C ring vibrations of polyamide. Upon membrane fouling, the following IR spectral changes may occur: (1) additional vibrational bands appear in the spectrum, (2) bands in the fingerprint region below 2000  $\text{cm}^{-1}$  become occluded, or (3) the relative band intensities are altered.

Generally speaking, the PACI/polyDADMAC-coagulated membranes are fouled to a lesser extent than the alum/polyDADMAC-coagulated membranes. The fouling layer for each of the PACI/polyDADMAC exposed membranes are less than 1  $\mu\text{m}$  thick as the underlying vibrational bands of the polyamide membrane are distinctly visible in the spectra (Figure 6). Infrared light must penetrate through the fouling layer before it reaches the membrane surface and reflects back when analyzed by the ATR method. The depth of penetration of the IR radiation is approximately 1  $\mu\text{m}$  at 1500  $\text{cm}^{-1}$ .

Table 3. Energy dispersive spectroscopy data from membrane surfaces

Element	Virgin Membrane	pH 7.9		pH 6.7		pH 7.8 & C <sub>6</sub> H <sub>8</sub> O <sub>7</sub>		pH 7.8, C <sub>6</sub> H <sub>8</sub> O <sub>7</sub> & AS
	--	Alum	PACl	Alum	PACl	Alum	PACl	Alum
O	71	49	50	50	49	49	65	47
Na	--	0.9	0.7	0.9	0.8	1.4	0.6	0.8
Mg	--	1.3	1.1	0.9	1.3	1.7	0.7	1.9
Al	--	18	16	15	16	18	16	27
Si	--	19	15	26	17	21	7.9	14
P	--	1.5	1.2	0.8	1.2	0.5	1.2	1.8
S	29	3.8	9.7	1.9	7.3	3.3	4.9	0.8
Cl	--	0.4	0.7	0.2	1.1	--	--	--
K	--	--	0.3	0.5	0.7	--	--	0.1
Ca	--	4.5	2.5	3.2	1.6	4.6	2.7	5.7
Ti	--	--	--	0.4	--	--	--	--
Fe	--	1.3	3.3	0.9	4.2	--	1.3	1.1

All data presented on a percent w/w basis.

AS = 3.0 mg/L Flocon 100 antiscalant.

The major component of the fouling layer is likely aluminum silicate (Al<sub>2</sub>Si<sub>2</sub>O<sub>5</sub>(OH)<sub>4</sub>) and silica (SiO<sub>2</sub>), as aluminum and silica are two of the major components of the EDS spectra (Table 3) [1]. Aluminum silicate in the form of kaolinite (equation 2) is comprised of 21 percent aluminum, 22 percent silica, 56 percent oxygen and 2 percent hydrogen on a percentage weight basis. The aluminum/silica ratios for most EDS samples match those for kaolinite closely. Notable exceptions are the samples containing citric acid (approximately 2:1 for the PACl and alum samples using citric acid). Citric acid was added for its binding ability for soluble aluminum. As such, citric acid may have altered the morphology of the foulant layer; as evidenced by (1) changes in aluminum/silica proportions in EDS data, (2) specific flux and salt rejection stabilization for alum-coagulated waters, and (3) lower differential pressures for alum-coagulated waters (Figure 5). Aluminum silicates also have characteristic vibrational bands at 3696, 3668, 3653, and 3620 cm<sup>-1</sup> (not shown in Figure 6) and an intense band between 1030 and 1020 cm<sup>-1</sup> [34]. Amorphous silica has characteristic vibrational bands at 1090, 790, and 475 cm<sup>-1</sup> [34].

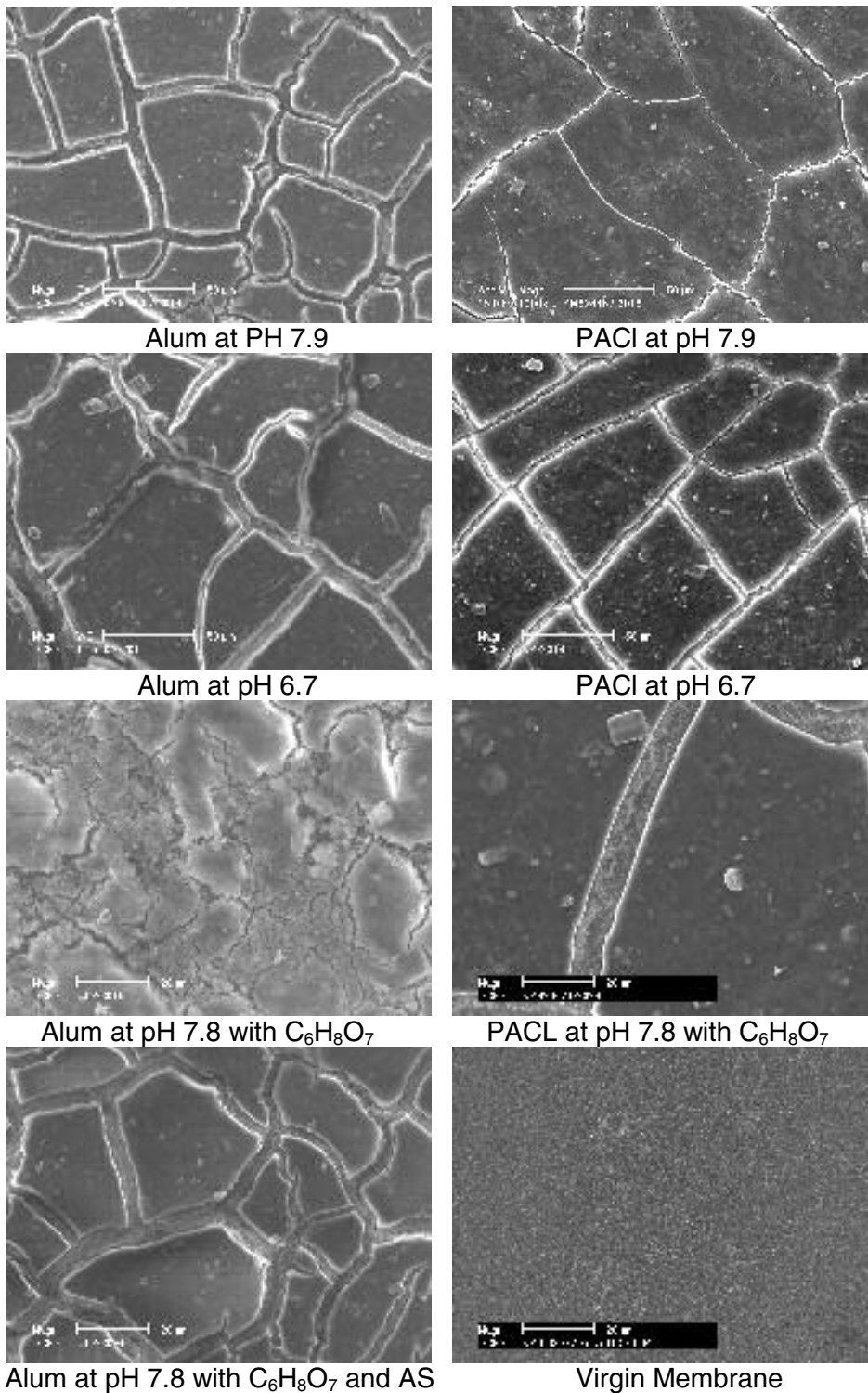


Figure 7. Scanning electron micrographs of fouled and virgin RO membranes:  
 1000X magnification. AS = Flocon 100 antiscalant

Of the three PACI/polyDADMAC membranes, increased fouling was seen for the membranes operated at pH 7.8 with citric acid, and pHs 6.7 and 7.9 without citric acid. However, each of the PACI/polyDADMAC-pretreated membranes showed minimal fouling and significantly less than those for alum pretreatment. The addition of citric acid to the feedwater resulted in significantly less membrane fouling, as interpreted by the increased intensity of the polyamide vibrational bands (1586, 1503, 1488, and 1243  $\text{cm}^{-1}$ ) in the fouled membrane spectrum (see Figure 6). As the intensity of polyamide/polysulfone vibrational bands increases, the degree of membrane fouling decreases. The EDS data supports this conclusion in that more sulfur—a major component of the polysulfone support layer—is present in the spectrum of the PACI-treated membranes (see Table 2).

Citric acid may contribute to the fouling layer. Figure 8 shows ATR/FT-IR difference spectra of PACI/polyDADMAC-pretreated polyamide membranes. For these membranes, the virgin membrane reference spectrum was subtracted from the fouled-membrane spectra. Major vibrational bands of citric acid are located near 1720  $\text{cm}^{-1}$  (carbonyl), 1574  $\text{cm}^{-1}$  (asymmetric  $\text{COO}^-$ ) and 1390  $\text{cm}^{-1}$  (symmetric  $\text{COO}^-$ ). The overlap of the asymmetric carboxylate with the amide I and amide II bands has the effect of shifting the location of the amide I band to lower wavenumber and the amide II to higher wavenumber. There is also a strong presence of the O-H stretching band and 1037  $\text{cm}^{-1}$  C-O stretching band, which is indicative of carbohydrates—possibly of biological origin.

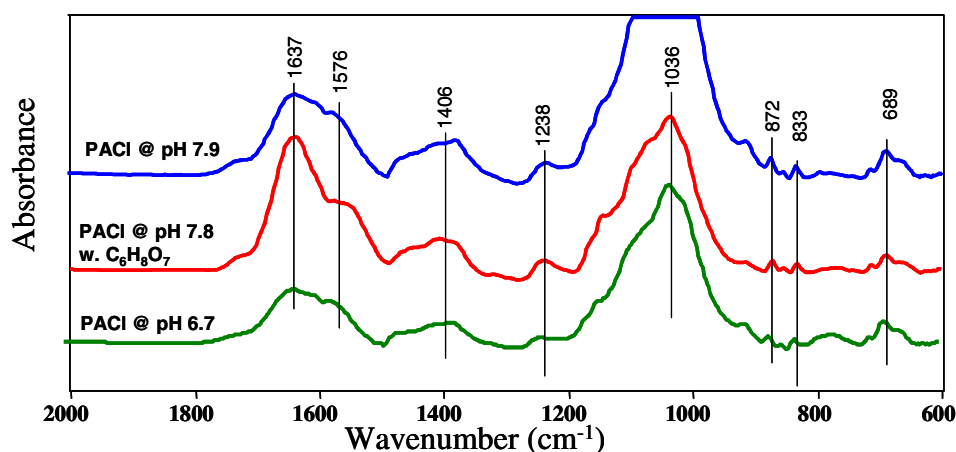


Figure 8. ATR/FT-IR difference spectra of PACI/polyDADMAC pretreated polyamide membranes

ATR/FT-IR spectra of the fouled reverse osmosis membranes using alum/polyDADMAC are also shown in Figure 6. The fouling layer is much heavier on the alum/polyDADMAC membranes compared to the PACI/polyDADMAC membranes, as all of the vibrational bands of the underlying membrane are totally obscured. The fouling layers appear to be well over 1  $\mu\text{m}$  thick. The pH adjustment of the alum/polyDADMAC feedwater produced little effect on the amount of material deposited. The spectra are similar to the fouling layer of PACI/polyDADMAC membrane; however, the broad band near 1010  $\text{cm}^{-1}$  dominates all four spectra. The weaker broad band near 668  $\text{cm}^{-1}$  in the spectra is actually an artifact. When the fouling layer is heavy and colloidal in composition, the absorbance spectra have a tendency to

“tail” upwards in intensity and then drop off near the frequency cutoff ( $\sim 600\text{ cm}^{-1}$ ) of the IR detector.

Vibrational bands associated with citric acid do not appear in the spectrum of the alum/polyDADMAC/citric acid membrane (Figure 6). However, weak vibrational bands at  $1553\text{ cm}^{-1}$ ,  $1452\text{ cm}^{-1}$  and  $1410\text{ cm}^{-1}$  do appear in the spectra of the PACl/polyDADMAC/citric acid and alum/polyDADMAC/citric acid/antiscalant membranes. These vibrational bands do not match the spectrum of the antiscalant, but there is a visual resemblance to the spectrum of a 5 percent w/v aqueous citric acid solution. The  $1553\text{ cm}^{-1}$  and  $1410\text{ cm}^{-1}$  may be associated with the asymmetric and symmetric carboxylate ( $\text{COO}^-$ ) stretching bands of citric acid. Complete deprotonation of the citric acid (i.e., all three carboxylic acids existing as carboxylates), various bound cations, or interaction with the antiscalant may significantly alter the citric acid spectrum. The foulants on these membranes do not appear to be biological in nature. No vibrational bands associated with the cationic polymer (polyDADMAC) were present in any of the fouled membrane spectra.

## CONCLUSIONS AND RECOMMENDATIONS

Many water utilities that could benefit from RO desalination already have conventional filtration facilities for particulate removal in place. However, data summarized here may indicate that water quality produced by these plants may not allow for proper downstream RO treatment. Aluminum residuals, most notably from alum coagulation, were observed to cause colloidal fouling of RO membranes through interactions with ambient silica to form aluminum silicates. Regardless of pH, the higher aluminum carryover for alum-coagulated waters caused severe membrane fouling within 500 hours of operation. Furthermore, these residuals may adversely react with various antiscalant chemicals used to mitigate sulfate-based precipitates. Only when a chelating agent (citric acid) was added to the alum-treated RO feed was the loss in productivity and selectivity arrested. A common alternative to alum is PACl, which minimizes colloidal fouling and may reduce aluminum-antiscalant interactions. However, the increase in water and salt passage under PACl-pretreatment conditions leads toward caution, as this testing showed that PACl in combination with  $\text{NH}_2\text{Cl}$  might also facilitate enhanced oxidation reactions on the polyamide membrane surface.

This paper was supported mostly through applied research. Given the limitations of each coagulant identified in this paper, more focused fundamental research is warranted. Specific recommendations for future work include research towards finding metal-compatible antiscalants, elucidating aluminum chemistry as it relates to chlorine tolerance of polyamide membranes, development of chlorine-tolerant membranes, and the evaluation of non-metal-based coagulants to remove turbidity prior to RO treatment.

## ACKNOWLEDGMENTS

This project was completed through the Desalination Research and Innovation Partnership with funding graciously provided by the California Energy Commission (contract # 400-00-013). Special thanks go to Milton Cox, Kevin Graff, Jerry Pitts, and the entire Water Quality Laboratory staff at MWDSC for their help on this project. Additional thanks are extended to Dr.

Krassimir Bozhilov at the University of California, Riverside, who conducted the SEM/EDS analyses.

## REFERENCES

1. Gabelich, C. J.; Yun, T. I.; Coffey, B. M.; Chen, W. R.; and Suffet, I. H. 2005. The Role of Dissolved Aluminum in Silica Chemistry for Membrane Processes. *Desalination* 180:307-319.
2. U.S. Environmental Protection Agency. 2003 (August 11). Long-Term 2 Enhanced Surface Water Treatment Rule. *Fed. Reg.* 68(154), 47640.
3. Office of Environmental Health Hazard Assessment. 1999 (October). *Draft Public Health Goal for Aluminum in Drinking Water*. California Environmental Protection Agency, Sacramento, Calif.
4. Wiesner, M. R., and Aptel, P. 1996. Mass Transport and Permeate Flux and Fouling in Pressure-Driven Processes. *Water Treatment: Membrane Processes* (J. Mallevalle, P. E. Odendaal, and M. R. Wiesner, eds.). McGraw-Hill, New York.
5. Letterman, R. D., and Driscoll, C. T. 1994. *Control of Residual Aluminum in Filtered Water*. AWWA, Denver, Colo.
6. Gabelich, C. J.; Yun, T. I.; Coffey, B. M.; and Suffet, I. H. 2002. Effects of Aluminum Sulfate and Ferric Chloride Coagulant Residuals on Polyamide Membrane Performance. *Desalination* 150(1), 15–30
7. Tchobanoglous, G., and Schroeder, E. D. 1985. *Water Quality*. Addison-Wesley, Boston.
8. Stumm, W., and Morgan, J. J. 1996. *Aquatic Chemistry: Chemical Equilibria and Rates in Natural Waters*, 3rd ed. John Wiley and Sons, New York.
9. Faust, S. D., and Aly, O. A. 1998. *Chemistry of Water Treatment*, 2nd ed. Ann Arbor Press, Ann Arbor, Mich.
10. American Society for Testing and Materials (ASTM). 1989. *Standard Practice for Calculation and Adjustment of Silica (SiO<sub>2</sub>) Scaling for Reverse Osmosis*, ASTM Designation D 4993–89. ASTM, Philadelphia.
11. Amjad, Z.; Zibrida, J. F.; and Zuhl, R. W. 1997. A New Antifoulant for Controlling Silica Fouling of Reverse Osmosis Systems. *Proceedings*, IDA World Congress on Desalination and Water Reuse, Madrid, Spain.
12. Metcalf and Eddy, Inc. 1991. *Wastewater Engineering: Treatment, Disposal, and Reuse*, 3rd ed. McGraw-Hill, New York.
13. Summit Research Labs (SRL). 2001. Commonly Asked Questions About Polyaluminum Chloride and Aluminum Chlorohydrate. SRL, Flemington, N.J.
14. Pernitsky, D. J., and Edzwald, J. K. 2000. Polyaluminum Chloride—Chemistry and Selection. AWWA Annual Conference and Exposition, Denver, Colo.
15. Bottero, J. Y.; Cases, J. M.; Fiessinger, F.; and Poirier, J. E. 1980. Studies of Hydrolyzed Aluminum Chloride Solutions: Nature of Aluminum Species and Composition of Aqueous Solutions. *J. Phys. Chem.* 84, 2933–2939.



16. Van Benschoten, J. E., and Edzwald, J. K. 1990. Chemical Aspects of Coagulation Using Aluminum Salts—I. Hydrolytic Reactions of Alum and Polyaluminum Chloride. *Wat. Res.* 24, 1519–1526.
17. Bertsch, P. M., and Parker, D. R. 1996. Aqueous Polynuclear Aluminum Species. *Environmental Chemistry of Aluminum* (G. Sposito, ed.). CRC Press, Boca Raton, Fla.
18. Bersillon, J.-L., and Thompson, M. A. 1996. Field Evaluation and Piloting. *Water Treatment: Membrane Processes* (J. Mallevalle, P. E. Odendaal, and M.R. Wiesner, eds.). McGraw-Hill, New York.
19. Boffardi, B. P. 1996. *Scale Deposit Control for Reverse Osmosis Systems*, Technical Bulletin No. 4–165. Calgon Corporation, Pittsburgh.
20. Drever, J. I. 1988. *The Geochemistry of Natural Waters*, 2nd ed. Prentice-Hall, Englewood, N.J.
21. Gabelich, C. J.; Zumarán, C. Y.; Cox, M. R.; Do, H.; and Pitts, J. L. 2002. Control of Residual Aluminum from Conventional Treatment to Improve Reverse Osmosis Performance. *Proceedings, 2002 AWWA Water Quality Technology Conference*, Seattle, Wash.
22. Gallup, D. L. 1997. Aluminum Silicate Scale Formation and Inhibition: Scale Characterization and Laboratory Experiments. *Geothermics*, 26(4), 483–499.
23. Norman, J. E.; Hoang, T.; and Leslie, G. L. 1999. Diagnosis and Remediation of Silicate Scale Fouling in Microfiltration Membranes: A Case Study. *Proceedings, 1999 AWWA Membrane Technology Conference*, Long Beach, Calif.
24. Gallup D. L. 1998. Aluminum Silicate Scale Formation and Inhibition (2): Scale Solubilities and Laboratory and Field Inhibition Tests. *Geothermics*, 27(4), 485–501.
25. American Society for Testing and Materials (ASTM). 1982. *Test Method for Silt Density Index*, Standard D4189–82. ASTM, Philadelphia.
26. American Society for Testing and Materials (ASTM). 1989. *Standard Practice for Standardizing Reverse Osmosis Performance Data*, ASTM Designation D 4516–85. ASTM, Philadelphia.
27. American Public Health Association (APHA), American Water Works Association, and Water Environment Federation. 1998. *Standard Methods for the Examination of Water and Wastewater*, 20th ed. (L. S. Clesceri, A. E. Greenberg, and A. D. Eaton, eds.). APHA, Washington, D.C.
28. Goldstein, J.; Newbury, D. E.; Echlin, P.; Joy, D. C.; Romig, A. D., Jr.; Lyman, C. E.; Fiori, C.; and Lifshin, E. 1992. *Scanning Electron Microscopy and X-Ray Microanalysis: A Text for Biologists, Materials Scientists, and Geologists*, 2nd Edition. Kluwer Academic/Plenum Publishers, New York.
29. Ridgway, H. F.; Ishida, K.; Rodriguez, G.; Safarik, J.; Knoell, T.; and Bold, R. 1998. Biofouling of Membranes I: Membrane Preparation and Characterization and Analysis of Bacterial Adhesion. *Methods of Enzymology*. R.J. Doyle, Louisville, Ky.
30. MWDSC. 2003. Unpublished data. Cooperative Research and Development Agreement with U.S. Bureau of Reclamation, Yuma, Ariz.

31. Hoek, E.M.V.; Kim, A. S.; and Elimelech, M. 2002. Influence of Crossflow Membrane Filter Geometry and Shear Rate on Colloidal Fouling in Reverse Osmosis and Nanofiltration Separations. *Env. Engrg. Sci.* 19(6), 357.
32. Hoek, E.M.V., and Elimelech, M. 2003. Cake-Enhanced Concentration Polarization: A New Fouling Mechanism for Salt-Rejecting Membranes. *Env. Sci. Technol.* 37(24):5581-5588.
33. Gabelich, C.J.; Franklin, J.C.; Geringer, F.W.; Ishida, K.P.; and Suffet, I.H. 2005. Enhanced Oxidation of Polyamide Membranes Using Monochloramine and Ferrous Iron. *J. Memb. Sci.* 258:64-70.
34. Craver, C. D. (ed.). 1982. *The Coblenz Society Desk Book of Infrared Spectra*, 2nd ed. The Coblenz Society, Kirkwood, Mo.